IEEE Access
Multidisciplinary ⋮ Rapid Review ⋮ Open Access Journal

Received October 14, 2021, accepted November 1, 2021, date of publication November 8, 2021,
date of current version November 19, 2021.

Digital Object Identifier 10.1109/ACCESS.2021.3125977

Design of an On-Glass 5G Monopole Antenna for a Vehicle Window Glass

DOYOUNG JANG[1], NAK KYOUNG KONG[2], AND HOSUNG CHOO[1], (Senior Member, IEEE)
[1]Department of Electronic and Electrical Engineering, Hongik University, Seoul 04066, South Korea
[2]Advanced Body Engineering Design Team, Hyundai Motor Company, Seoul 137-938, South Korea

Corresponding author: Hosung Choo (hschoo@hongik.ac.kr)

This work was supported in part by Hyundai Motor Company, in part by the Basic Science Research Program through the National Research Foundation of Korea (NRF) funded by the Ministry of Education under Grant NRF-2017R1A5A1015596, and in part by the NRF Grant funded by the Korea Government under Grant 2015R1A6A1A03031833.

ABSTRACT In this paper, we propose a design for an on-glass 5G monopole antenna for a vehicle window glass. The proposed antenna consists of a monopole resonator, an inductive line, and a co-planar waveguide (CPW), which can adjust the phase so that the current in each resonator is close to in phase. Therefore, although the vehicle window glass has a high dielectric loss, the proposed monopole with an inductive line can obtain an antenna gain that is suitable for applying to vehicle 5G communications. To verify the antenna characteristics, the reflection coefficients and the radiation patterns are measured in a full anechoic chamber. The results demonstrate that the proposed on-glass antenna is suitable for applying in vehicle 5G communications.

INDEX TERMS Antennas, antenna arrays, glass products, glass antennas, 5G antennas, autonomous driving.

I. INTRODUCTION

Recently, the demand has been progressively increasing for a vehicle-to-everything (V2X) communication technology to improve the level of autonomous driving technology [1]–[4]. V2X typically encompasses several specific technologies such as vehicle-to-vehicle (V2V), vehicle-to-pedestrian (V2P), vehicle-to-infrastructure (V2I), and vehicle-to-network (V2N), which can improve the safety and efficiency of autonomous driving. However, due to limited data throughput and latency issues, previous communication technologies are not suitable for V2X. Notably, 5G communication systems that use a millimeter wave (mmWave) have numerous advantages, such as low latency, high speed, and high capacity. Therefore, attempts to apply 5G communication techniques in autonomous vehicles have been increasing [5]–[7]. To apply 5G techniques to an autonomous vehicle, a high-gain 5G array antenna must be mounted on a small area of the vehicle. To address concerns regarding the appearance and air resistance of the vehicle, a shark-fin is generally used on the roof of the automobile for various vehicle antennas [8]–[10]. However, since a number of antennas (e.g., DMB, GPS, and LTE) are already built-in in the shark-fin housing, there is not enough space to insert an additional high-gain 5G array antenna without performance degradation from mutual coupling effect with adjacent antennas. To reduce the mutual coupling characteristics, various techniques such as the use of a cavity wall [11], a meta-surface [12], and a resonator [13] have been introduced. Nevertheless, the space is still not enough to insert these isolators in the shark-fin housing. In comparison, a glass antenna technique that prints an antenna pattern on the vehicle window has several significant advantages. First, the glass antenna does not require additional mounting space, which can preserve the appearance of the vehicles. Second, printing the antenna on the window glass prevents physical and electrical interferences (blockage or mutual coupling) with other vehicle antennas. Finally, the glass antenna can be easily made within the manufacturing process of the vehicle window glass. For these reasons, a glass antenna can be considered as a noteworthy candidate antenna type for applying in vehicle wireless communications, although thick glass windows with high dielectric loss characteristics does not help the performance of the 5G antenna at all. However, the previous studies on vehicle window glass antennas are limited in low frequency bands such as AM/FM, DMB, LTE, and 5G sub-6 band [14]–[16]. Although some studies on glass antennas have been attempted at a high frequency in the mmWave band, they were conducted on very thin glass, less than 0.5 mm [17]–[19]. Similarly, printed 5G

The associate editor coordinating the review of this manuscript and approving it for publication was Tutku Karacolak.

antennas of general types such as Vivaldi antennas [20], slot antennas [21], and dipole antennas [22] do not consider glass substrates with high dielectric loss characteristics. In reality, the laminated glass for vehicle windshields with electrically very thick thickness has a high dielectric loss in the 5G mmWave band [23]–[25]. Therefore, in-depth research on a 5G antenna design for electrically thick window glass is required.

In this paper, we propose a design for an on-glass 5G monopole antenna for vehicle window glass. The proposed antenna consists of a monopole resonator, an inductive line, and a co-planar waveguide (CPW). The inductive line connecting the monopole resonators can adjust the phase so the current in each resonator is close to the in-phase. Therefore, although the vehicle window glass has a high dielectric loss, the proposed monopole with an inductive line can obtain an antenna gain that is suitable for applying to vehicle 5G communications. The monopole antenna is fed through a CPW transmission line. Herein, the monopole array and the CPW use only a single layer of vehicle window; therefore, it can be fabricated through a simple manufacturing process. Taking the smooth surface of the vehicle window glass into consideration, the conducting antenna body is attached using a thermosetting adhesive. To verify the antenna characteristics, the reflection coefficients and the radiation patterns are measured in a full anechoic chamber. The results demonstrate that the proposed on-glass antenna is suitable for applying in vehicle 5G communications.

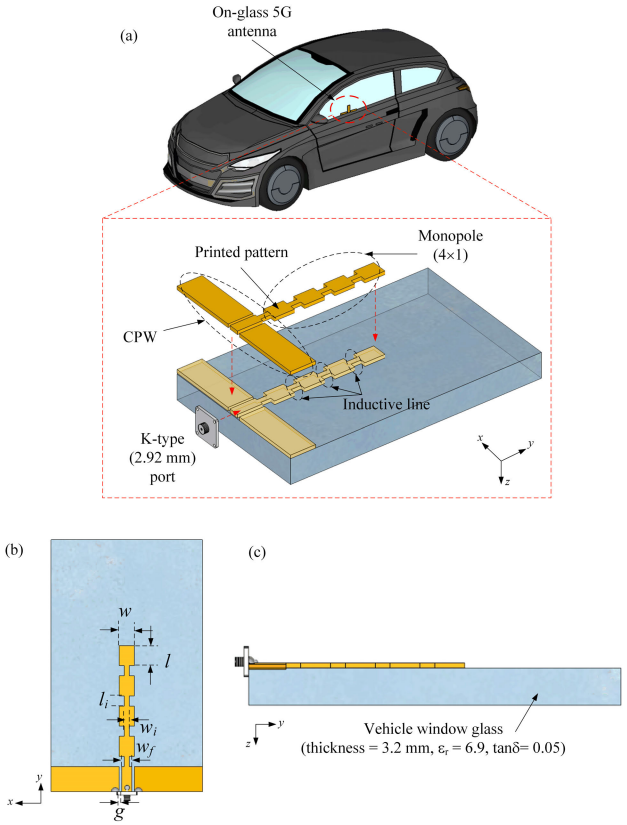

FIGURE 1. Geometry of the proposed antenna. (a) isometric view. (b) bottom view. (c) side view.

II. DESIGN OF THE PROPOSED ANTENNA

Figure 1 illustrates the geometry of the on-glass 5G monopole antenna for vehicle window glass. The proposed antenna is attached to the side of the vehicle window glass, as shown in Figure 1(a). This window glass has a high dielectric loss characteristic ($\varepsilon_r = 6.95$, $tan\delta = 0.05$) with an electrically thick thickness of 3.2 mm. Therefore, it is difficult to obtain a suitable antenna gain with a 1/4 wavelength conventional printed antenna. To improve the antenna gain while simultaneously considering the high loss characteristics of the vehicle window glass, the proposed antenna consists of 4 × 1 monopole resonators with width and length of w and l, respectively. The monopole resonators are connected through the inductive line with width and length of w_i and l_i, respectively. The inductive line can adjust the phase of each resonator, making the surface current in each resonator close to the in-phase. Herein, the total radiation pattern of the 4 × 1 monopole resonators with the inductive lines can be expressed as follows:

$$X_{4\times1} = \sum_{n=1}^{N} F_n(\theta) e^{jkd\cdot\sin\theta\cdot\phi_{opt}} \tag{1}$$

where F_n is the radiation pattern of the nth single resonator ($n = 1, 2, 3, 4$), k is the wave number, and d is the array spacing. In addition, 'ϕ_{opt} is the phase delay by the optimized inductive line that can makes the surface current in each resonator close to the in-phase. In an ideal situation, the 4 × 1 monopole resonators with perfect in-phase state for each resonator have a higher gain of 6 dB than a single monopole resonator. Moreover, to obtain a higher antenna gain, the 4 × 1 monopole can repeatedly arrange in the x-axis direction. For example, the radiation pattern of the 4 × 4 monopole array expresses as the summation of $X_{4\times1n}$ as follows:

$$X_{4\times4} = \sum_{n=1}^{N} X_{4\times1n}(\theta) e^{jkd\cdot\sin\theta} \tag{2}$$

Likewise, the 4 × 4 monopole array gain is higher of 6 dB than the 4 × 1 monopole array in an ideal situation. Therefore, although a vehicle window has a high dielectric loss characteristic, the proposed antenna can obtain the antenna gain suitable for applying 5G communications The proposed antenna is linearly polarized, which is widely employed in vehicle 5G communications because it has some advantages such as ease of an antenna design and fabrication [26]–[29]. An input signal is fed to the proposed antenna through the CPW line with a width of w_f and a gap of g. Since the monopole resonators and the CPW use only a single layer of vehicle window, it can be fabricated through a simple manufacturing process. The detailed design parameters for maximizing the bore-sight gain are obtained

TABLE 1. Optimized values of the proposed antenna.

Parameters	Value (mm)
w	1.8
l	2.8
l_i	0.7
w_i	0.4
w_f	0.5
g	0.13

with the FEKO electromagnetic (EM) simulator [30]–[33]. The optimized values are listed in Table 1.

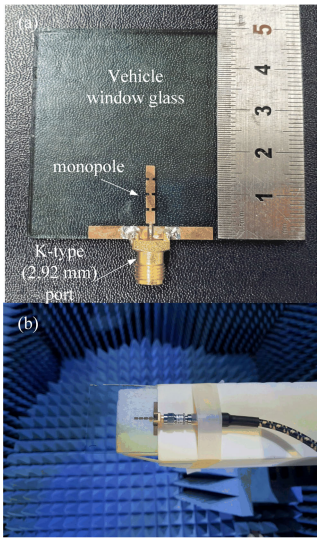

FIGURE 2. Photograph of the proposed antenna. (a) fabricated antenna. (b) measurement setup.

Figure 2 presents a photograph of the fabricated 4 × 1 monopole antenna. In general, since vehicle windows have very smooth surfaces, it is difficult to deposit a copper layer on the glass substrate. Therefore, the glass antenna cannot be fabricated using the usual method for printed antennas. To print the conducting antenna body on the vehicle window, a silk screen method is used in general. However, this method has poor manufacturing tolerance, so it is not suitable for fabricating 5G antennas with small antenna patterns. To solve these manufacturing problems, a thermosetting adhesive is used to attach a copper film on the vehicle window glass. The thermosetting adhesive can maintain adhesion between the glass and the antenna body when the antenna pattern is heated for the soldering process. At the next stage, the vehicle window with an attached copper film is etched, which makes it possible to form a small antenna pattern despite the fact that the vehicle window glass has a smooth surface. A part of the CPW line is connected to a K-type (2.92 mm) port that can operate the antenna with a low insertion loss at the 5G mmWave band. To verify the fabricated antenna, the reflection coefficients and the radiation patterns are measured in a full anechoic chamber.

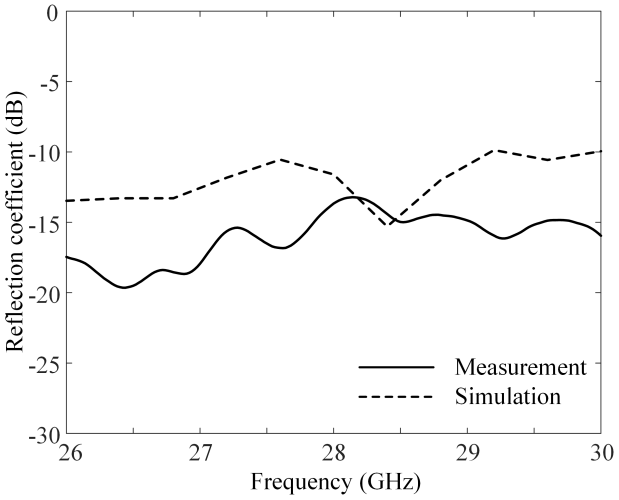

FIGURE 3. Reflection coefficients of the proposed antenna.

Figure 3 presents the reflection coefficients of the proposed antenna. The solid and dashed lines indicate the measured and the simulated reflection coefficients, respectively. The measured reflection coefficient maintains a value that is less than −10 dB in the observed frequency band, which is in good agreement with the simulated results. Therefore, the proposed antenna can be used in the 5G mmWave band.

Figure 4 shows the 2-D radiation patterns of the proposed antenna on the *zx*- and *zy*- planes. The measured and simulated co-polarization gains (bore-sight direction) are 0 dBi and 0.4 dBi at 28 GHz. The gain of the proposed antenna is not higher than that of conventional monopole antennas, because the high dielectric loss of the commercial vehicle glass causes the decrement of the radiation efficiency. In fact, the proposed antenna has a low radiation efficiency of 11.1% at 28 GHz. Of course, if the proposed antenna is designed with a low loss substrate, then the antenna gain can be enhanced as much for the conventional monopoles. On the other hand, the cross-polarization gain (bore-sight direction) is −20.1 dBi, which means that the proposed antenna has linear polarization characteristics. In addition, the half power beamwidths (HPBWs) are 18° (*zx*-plane) and 27° (*zy*-plane), which shows good agreement in comparison to the simulated HPBWs of 14° (*zx*-plane) and 29° (*zy*-plane). To verify the feasibility, the antenna characteristics such as an operating frequency band, a maximum gain, antenna dimensions, and a substrate material of the proposed antenna are compared to those in other previous studies, as listed in Table 2.

III. VERIFICATION OF THE PROPOSED ANTENNA

To verify the operating principles of the proposed on-glass antenna, the 5G monopole antenna is analyzed from a circuit perspective. Figure 5 indicates an equivalent circuit model for the proposed 4 × 1 monopole antenna. The equivalent circuit model is obtained using a data fitting method. Herein, R_n, L_n, and C_n indicate the resistance, inductance, and capacitance

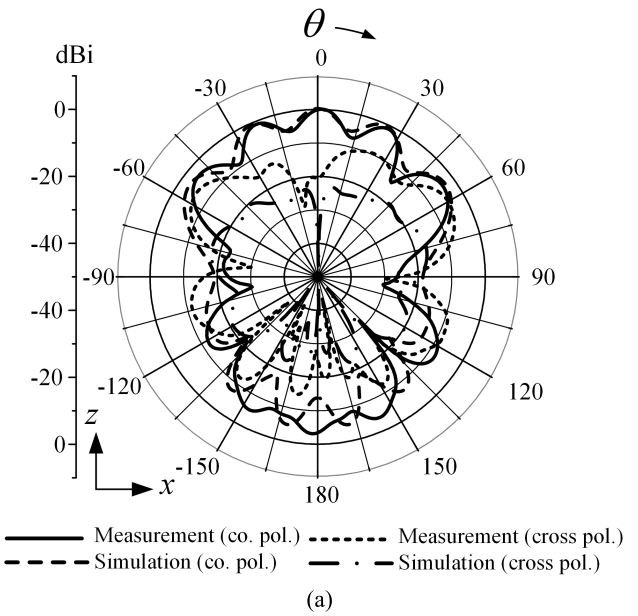

(a)

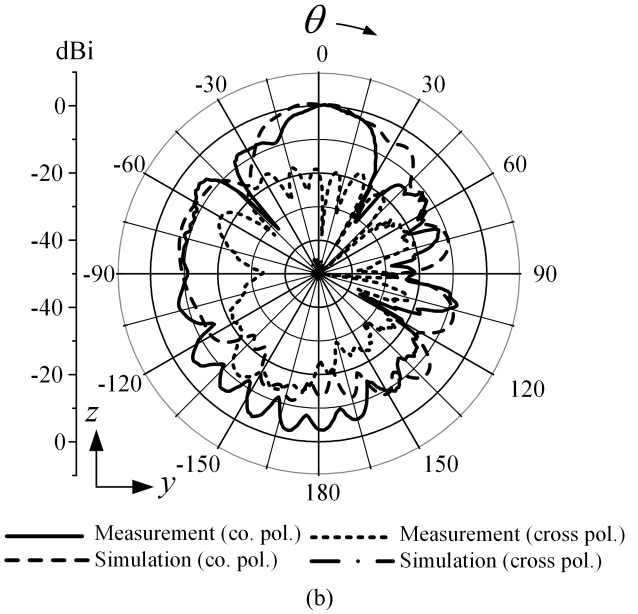

(b)

FIGURE 4. 2-D radiation patterns at 28 GHz. (a) zx-plane. (b) zy-plane.

TABLE 2. Comparisons of antenna characteristics.

Research	Operating band	Maximum gain	Antenna Size	Substrate
[15]	88-106 MHz	-	52.6 cm (width)	Glass
[16]	4.66-11.84 GHz	–0.15 dBi	50 × 17 × 1 mm^3	Glass
[20]	24-30.6 GHz	> 5 dBi	40 × 24 × 1.6 mm^3	FR-4
[21]	25-30 GHz	> 8 dBi	20 × 16 × 0.508 mm^3	Nelco NY9220
[22]	112.5-130 MHz	–7.58 dBi	1.2 × 0.42 m^2	
Proposed antenna	26-30 GHz	5 dBi	50 × 50 × 3.2 mm^3	Glass

components of the nth resonator ($n = 1, 2, 3, 4$), while L_f is the feed inductance. The mth inductive line from the source

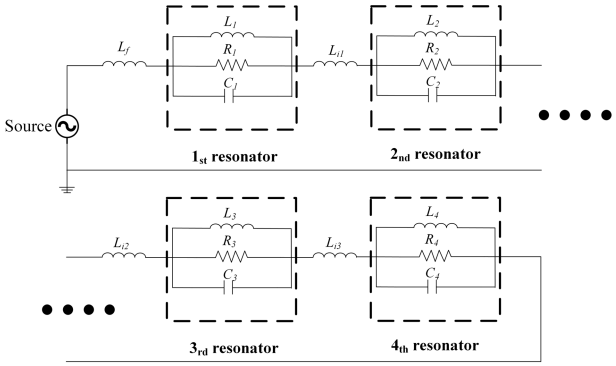

FIGURE 5. Equivalent circuit model.

TABLE 3. Values of the equivalent circuit model.

Parameters	Value	Parameters	Value
L_f	100 pH	R_1	128 Ω
C_1	1.6 pF	L_1	16 pH
R_2	188 Ω	C_2	582 fF
L_2	75 pH	R_3	248 Ω
C_3	102 fF	L_3	920 pH
R_4	26 Ω	C_4	2.9 pF
L_4	9.0 pH	L_{i1}	240 pH
L_{i2}	240 pH	L_{i3}	240 pH

connecting the monopole resonator is specified as $L_{im}(m = 1, 2, 3)$. The parameters of each lumped element are adjusted iteratively to minimize the impedance difference between the circuit model and the full EM simulation. The results are compared in Figure. 6. The detailed parameters of the lumped elements are listed in Table 3.

Figure 6 shows a comparison of the impedance characteristics of the equivalent circuit model and the full EM simulated model, including their parametric studies. To clearly examine the operating principles of the 4 × 1 monopole antenna with an inductive line, in the comparison, the full EM simulation model does not include a substrate. In Figure 6(a), the solid and dashed lines indicate the real and imaginary parts of the impedance characteristics of the equivalent circuit model, while the dotted and dash-dotted lines are the results of full EM simulated model. The tendency of the impedance characteristics of the equivalent circuit model is in good agreement with the full EM simulation results, as shown in Figure 6(a). When the inductance of L_{im} is changed from 90 to 240 pH, the reactance of the equivalent circuit model is enhanced, as shown in Figure 6(b). In comparison, when the length of the inductive lines l_i are varied from 0.1 to 0.4 mm, the reactance characteristics are improved, as shown in Figure 6(c). This result is similar to that demonstrated in Figure 6(b).

Figure 7 represents the surface current phase variance of the monopole antenna with inductive lines (case 1) and without the inductive lines (case 2). The length of case 1 is the same as the total length of case 2, as shown in Figure 7(a). The surface current phase is examined along the resonator

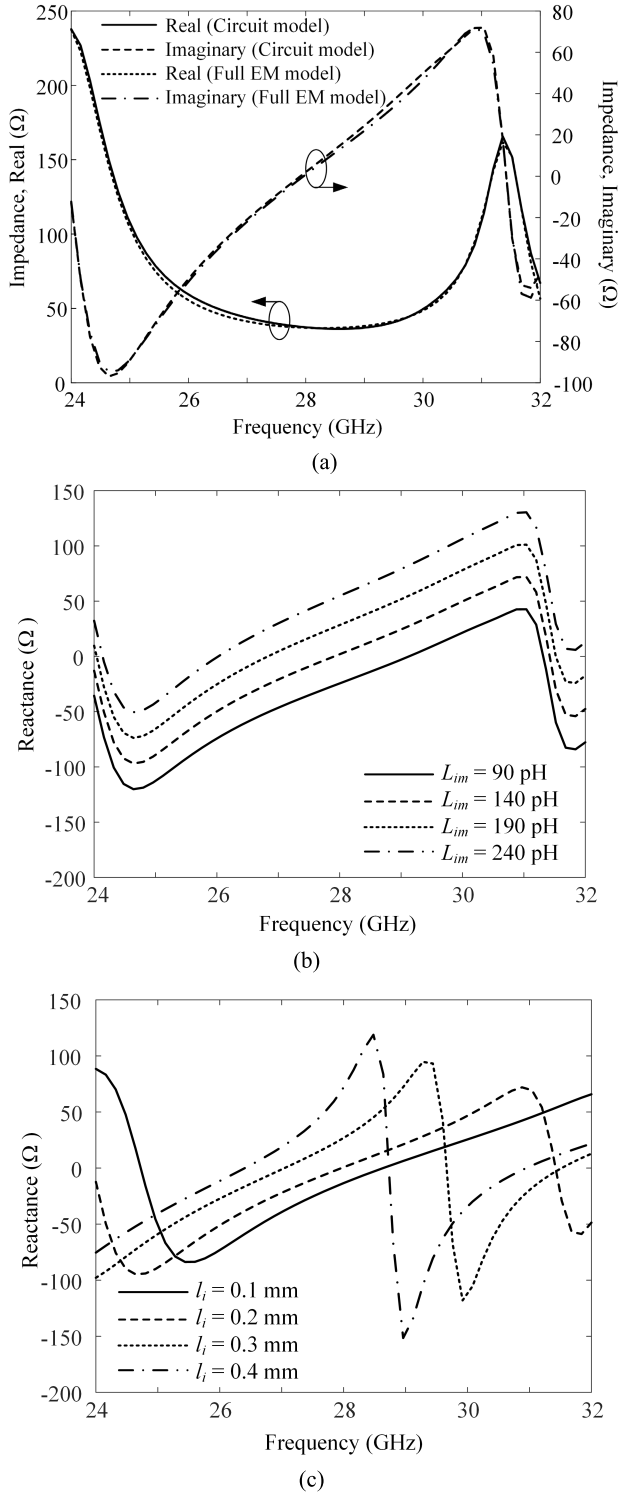

FIGURE 6. Impedance characteristics of equivalent circuit model and full EM simulated model. (a) comparison of impedance characteristics. (b) parametric study of L_{im}. (c) parametric study of l_i.

edge lines of each case. The surface current phase in case 1, indicated by the solid line, is close to the in-phase, as shown in Figure 7(b). However, the phase in case 2 (dashed line) cannot maintain the in phase. The results indicate that inductive lines

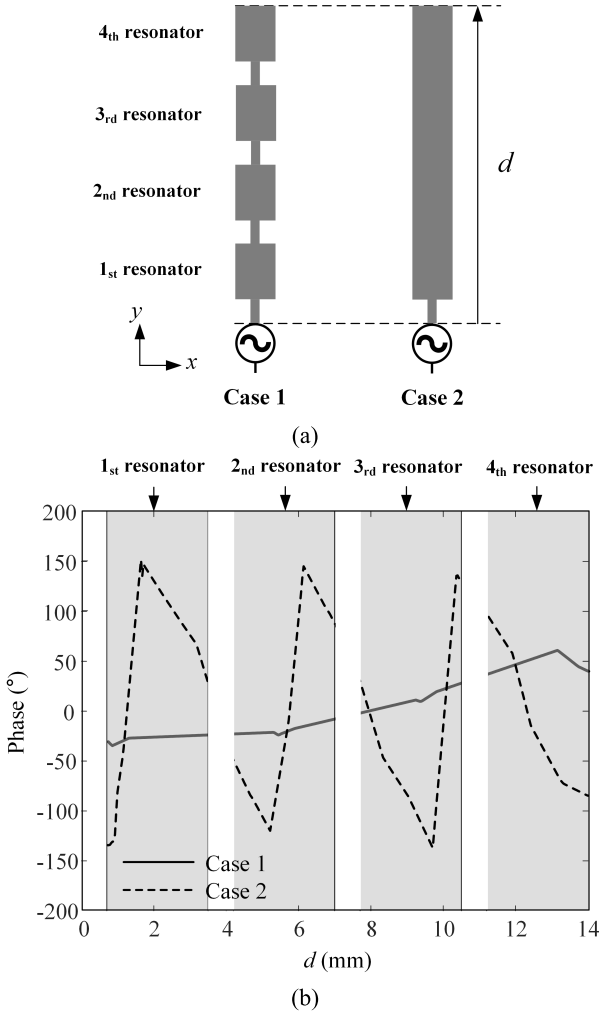

FIGURE 7. Phase variance of the surface current with and without an inductive line. (a) two cases. (b) their phase variances.

are required to improve the gain by adjusting the surface current phase of the resonators.

Figure 8 illustrates the geometry and photograph of the expanded 4 × 4 array configuration that can obtain enhanced bore-sight gain than the 4 × 1 monopole. For this configuration, the 4 × 1 monopole is repeatedly arranged in the x-axis direction, and the array spacing is determined to be 8.4 mm. The 4 × 4 array antenna is manufactured using the same methods described in Figure 2. The fabricated 4 × 4 array antenna is measured in a full anechoic chamber to obtain the radiation patterns of the array antenna.

Figure 9 shows the 2-D radiation pattern of the proposed 4 × 4 array antenna on the zx-plane. The solid and dashed lines indicate the measured and the simulated radiation patterns. The bore-sight gains of the measured and the simulated are 5.1 dBi and 3.9 dBi at 28 GHz, respectively. It shows a 5.1 dB higher gain than the 4 × 1 array configuration, which is good agreement with the theoretically expected result. In addition, the HPBW is 11.5°, which shows good agreement with the simulated HPBW of 15°.

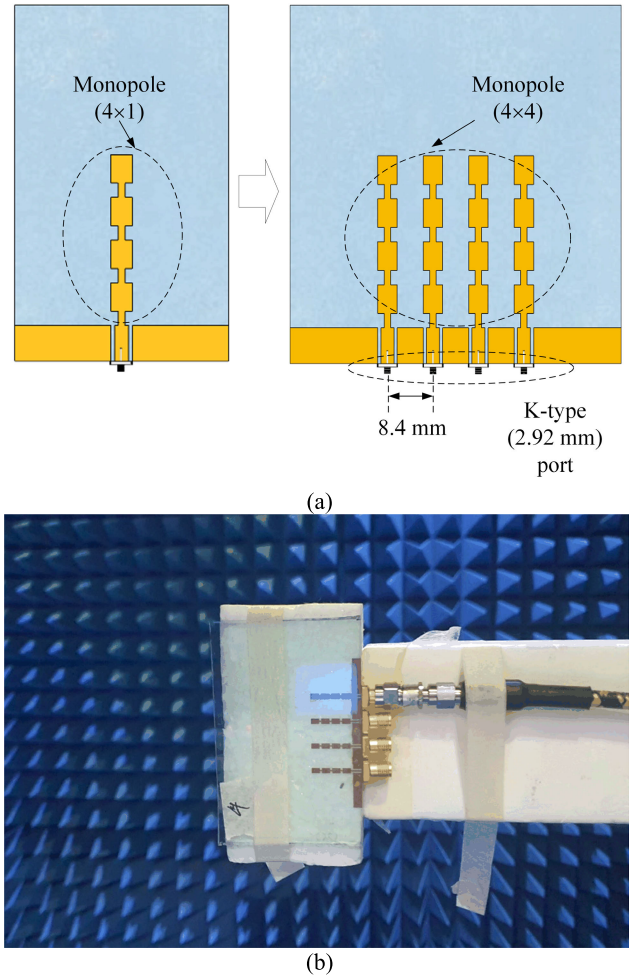

FIGURE 8. 4 × 4 array configuration. (a) array geometry. (b) fabricated array.

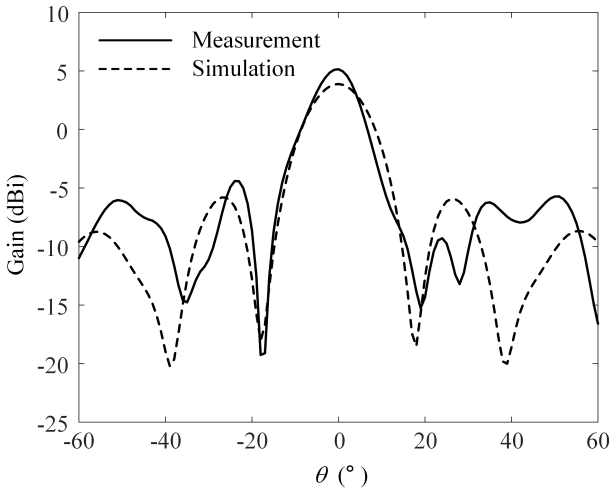

FIGURE 9. Radiation patterns of the 4 × 4 proposed array on the zx-plane.

IV. CONCLUSION

We investigated the design of the on-glass 5G monopole antenna for the vehicle window glass. The proposed antenna consisted of the monopole resonator, the inductive line, and the CPW. The inductive line connecting the monopole resonators, could adjust the phase so that the current in each resonator was close to in phase. Therefore, although the vehicle window glass had the high dielectric loss, the proposed monopole with the inductive line could obtain the antenna gain suitable for applying to vehicle 5G communications. To verify the antenna characteristics, the reflection coefficients and the radiation patterns were measured in the full anechoic chamber. The measured reflection coefficient remained at less than −10 dB in the 5G mmWave band. In addition, when the array antenna was in the 4 × 4 configuration, the measured bore-sight gain and HBPW were 5.1 dBi and 11.5° at 28 GHz, respectively. To analyze the operating principle of the proposed on-glass 5G monopole antenna, the imaginary characteristics of impedance were examined for the equivalent circuit model and the full EM simulation model. In addition, the surface current phase variance of the monopole antenna was observed and compared both with and without the inductive line. The results demonstrated that the inductive lines were required to improve the gain by adjusting the surface current phase of the resonators. On the other hand, the proposed antenna had the small size but not optically transparent. To enhance the visibility, transparent conductors or mesh structures can be applied to 5G glass antenna in future work.

REFERENCES

[1] G. Naik, B. Choudhury, and J.-M. Park, "IEEE 802.11bd & 5G NR V2X: Evolution of radio access technologies for V2X communications," *IEEE Access*, vol. 7, pp. 70169–70184, 2019.

[2] S. Chen, J. Hu, Y. Shi, L. Zhao, and W. Li, "A vision of C-V2X: Technologies, field testing, and challenges with Chinese development," *IEEE Internet Things J.*, vol. 7, no. 5, pp. 3872–3881, May 2020.

[3] A. Moubayed, A. Shami, P. Heidari, A. Larabi, and R. Brunner, "A vision of C-V2X: Technologies, field testing, and challenges with Chinese development," *IEEE Trans. Mob. Comput.*, vol. 20, no. 4, pp. 1380–1392, Apr. 2021.

[4] K. Abboud, H. A. Omar, and W. Zhuang, "Interworking of DSRC and cellular network technologies for V2X communications: A survey," *IEEE Trans. Veh. Technol.*, vol. 65, no. 12, pp. 9457–9470, Dec. 2016.

[5] A. Ghosh, A. Maeder, M. Baker, and D. Chandramouli, "5G evolution: A view on 5G cellular technology beyond 3GPP release 15," *IEEE Access*, vol. 7, pp. 127639–127651, 2019.

[6] H. Ma, S. Li, E. Zhang, Z. Lv, J. Hu, and X. Wei, "Cooperative autonomous driving oriented MEC-aided 5G-V2X: Prototype system design, field tests and AI-based optimization tools," *IEEE Access*, vol. 8, pp. 54288–54302, 2020.

[7] C. R. Storck and F. Duarte-Figueiredo, "A survey of 5G technology evolution, standards, and infrastructure associated with vehicle-to-everything communications by Internet of Vehicles," *IEEE Access*, vol. 8, pp. 117593–117614, 2020.

[8] Y. Liu, Z. Ai, G. Liu, and Y. Jia, "An integrated shark-fin antenna for MIMO-LTE, FM, and GPS applications," *IEEE Antennas Wireless Propag. Lett.*, vol. 18, no. 8, pp. 1666–1670, Aug. 2019.

[9] O.-Y. Kwon, B.-S. Kim, and R. Song, "A fully integrated shark-fin antenna for MIMO-LTE, GPS, WLAN, and WAVE applications," *IEEE Antennas Wireless Propag. Lett.*, vol. 17, no. 4, pp. 600–603, Mar. 2018.

[10] D. Rongas, A. Paraskevopoulos, L. Marantis, and A. G. Kanatas, "An integrated shark-fin reconfigurable antenna for V2X communications," *Prog. Electromagn. Res.*, vol. 100, pp. 1–16, 2020.

[11] J. Hur and H. Choo, "Design of a small array antenna with an extended cavity structure for wireless power transmission," *J. Electromagn. Eng. Sci.*, vol. 20, no. 1, pp. 9–15, Jan. 2020.

[12] M.-C. Tang, Z. Chen, H. Wang, M. Li, B. Luo, J. Wang, Z. Shi, and R. W. Ziolkowski, "Mutual coupling reduction using meta-structures for wideband, dual-polarized, and high-density patch arrays," *IEEE Trans. Antennas Propag.*, vol. 65, no. 8, pp. 3986–3998, Aug. 2017.
[13] K. S. Vishvaksenan, K. Mithra, R. Kalaiarasan, and K. S. Raj, "Mutual coupling reduction in microstrip patch antenna arrays using parallel coupled-line resonators," *IEEE Antennas Wireless Propag. Lett.*, vol. 16, pp. 2146–2149, 2017.
[14] S. Ahn, Y. S. Cho, and H. Choo, "Diversity on-glass antennas for maximized channel capacity for FM radio reception in vehicles," *IEEE Trans. Antennas Propag.*, vol. 59, no. 2, pp. 699–702, Feb. 2011.
[15] J. Schaffner, H. Song, A. Bekaryan, H.-P. Hsu, M. Wisnewski, and J. Graham, "The impact of vehicle structural components on radiation patterns of a window glass embedded FM antenna," *IEEE Trans. Antennas Propag.*, vol. 59, no. 10, pp. 3536–3543, Oct. 2011.
[16] J. I. Trujillo-Flores, R. Torrealba-Meléndez, J. M. Muñoz-Pacheco, M. A. Vásquez-Agustín, E. I. Tamariz-Flores, E. Colín-Beltrán, and M. López-López, "CPW-fed transparent antenna for vehicle communications," *Appl. Sci.*, vol. 10, no. 17, p. 6001, Aug. 2020.
[17] N. Ranjkesh, A. Taeb, S. Gigoyan, M. Basha, and S. S. Naeini, "Millimeter-wave silicon-on-glass integrated tapered antenna," *IEEE Antennas Wireless Propag. Lett.*, vol. 13, pp. 1425–1428, 2014.
[18] A. O. Watanabe, T. H. Lin, M. Ali, Y. Wang, V. Smet, P. M. Raj, M. M. Tentzeris, R. R. Tummala, and M. Swaminathan, "Ultrathin antenna-integrated glass-based millimeter-wave package with through-glass vias," *IEEE Trans. Microw. Theory Techn.*, vol. 68, no. 12, pp. 5082–5092, Dec. 2020.
[19] A. H. Naqvi, J.-H. Park, C.-W. Baek, and S. Lim, "V-band end-fire radiating planar micromachined helical antenna using through-glass silicon via (TGSV) technology," *IEEE Access*, vol. 7, pp. 87907–87915, 2019.
[20] A. S. Dixit and S. Kumar, "The enhanced gain and cost-effective antipodal Vivaldi antenna for 5G communication applications," *Microw. Opt. Technol. Lett.*, vol. 62, no. 6, pp. 2365–2374, Jun. 2020.
[21] G. S. Karthikeya, M. P. Abegaonkar, and S. K. Koul, "A wideband conformal antenna with high pattern integrity for mmWave 5G smartphones," *Prog. Electromagn. Res. Lett.*, vol. 84, pp. 1–6, 2019.
[22] S. X. Ta, H. Choo, and I. Park, "Broadband printed-dipole antenna and its arrays for 5G applications," *IEEE Antennas Wireless Propag. Lett.*, vol. 16, pp. 2183–2186, 2017.
[23] C. R. White, H. J. Song, and E. Yasan, "A wideband stick-on connector for CPW-fed on-glass antennas," *IEEE Antennas Wireless Propag. Lett.*, vol. 9, pp. 171–174, 2010.
[24] S. Ahn and H. Choo, "A systematic design method of on-glass antennas using mesh-grid structures," *IEEE Trans. Veh. Technol.*, vol. 59, no. 7, pp. 3286–3293, Sep. 2010.
[25] R. Oven and P. R. Young, "Microwave loss of coplanar waveguides on electrically ion depleted borosilicate glass," *IEEE Microw. Wireless Compon. Lett.*, vol. 15, no. 2, pp. 125–127, Feb. 2005.
[26] B. Feng, J. Chen, S. Yin, C.-Y.-D. Sim, and Z. Zhao, "A tri-polarized antenna with diverse radiation characteristics for 5G and V2X communications," *IEEE Trans. Veh. Technol.*, vol. 69, no. 9, pp. 10115–10126, Sep. 2020.
[27] S. Gao, L. Ge, D. Zhang, and W. Qin, "Low-profile dual-band stacked microstrip monopolar patch antenna for WLAN and car-to-car communications," *IEEE Access*, vol. 6, pp. 69575–69581, 2018.
[28] P. A. Dzagbletey, J.-Y. Shim, and J.-Y. Chung, "Quarter-wave balun fed Vivaldi antenna pair for V2X communication measurement," *IEEE Trans. Antennas Propag.*, vol. 67, no. 3, pp. 1957–1962, Mar. 2019.
[29] H. Wong, K. K. So, and X. Gao, "Bandwidth enhancement of a monopolar patch antenna with V-shaped slot for car-to-car and WLAN communications," *IEEE Trans. Veh. Technol.*, vol. 65, no. 3, pp. 1130–1136, Mar. 2016.
[30] R. L. Haupt and S. E. Haupt, *Practical Genetic Algorithms*, 2nd ed. New York, NY, USA: Wiley, 2004.
[31] T. Yu, H. Lee, S.-J. Park, and S. Nam, "A uniform heating technique for cavity in volatile organic compound (VOC) removal system using slotted waveguide array," *J. Electromagn. Eng. Sci.*, vol. 21, no. 2, pp. 126–133, Apr. 2021.
[32] D. Jang, J. Hur, H. Shim, J. Park, C. Cho, and H. Choo, "Array antenna design for passive coherent location systems with non-uniform array configurations," *J. Electromagn. Eng. Sci.*, vol. 20, no. 3, pp. 176–182, Jul. 2020.
[33] Altair Engineering Inc. (Jul. 1, 2021). *FEKO EM Simulation Software*. [Online]. Available: http://www.altair.co.kr

DOYOUNG JANG received the B.S. degree in information and telecommunication engineering from Dongyang Mirae University, Seoul, South Korea, in 2018, and the M.S. degree in electronic and electrical engineering from Hongik University, Seoul, in 2020, where he is currently pursuing the Ph.D. degree in electronic and electrical engineering. He worked as a Research Engineer with MOASOFT, Seoul, from 2015 to 2018. His research interests include direction finding, passive radar, electromagnetic wave propagation, and electromagnetic environmental effects.

NAK KYOUNG KONG received the B.S. degree in mechanical engineering from Hongik University, Seoul, in 2003. He is currently a Senior Research Engineer with Hyundai Motor Company. He is in charge of advanced technology of body parts.

HOSUNG CHOO (Senior Member, IEEE) received the B.S. degree in radio science and engineering from Hanyang University, Seoul, South Korea, in 1998, and the M.S. and Ph.D. degrees in electrical and computer engineering from The University of Texas at Austin, in 2000 and 2003, respectively. In September 2003, he joined the School of Electronic and Electrical Engineering, Hongik University, Seoul, where he is currently a Professor. His research interests include electrically small antennas for wireless communications, reader and tag antennas for RFID, on-glass and conformal antennas for vehicles and aircraft, and array antennas for GPS applications.